




## Singularly perturbed two-point boundary value problem by applying exponential fitted finite difference method

N. Kumar\*, R. Kumar Sinha and R. Ranjan 

### Abstract

The present study addresses an exponentially fitted finite difference method to obtain the solution of singularly perturbed two-point boundary value problems (BVPs) having a boundary layer at one end (left or right) point on uniform mesh. A fitting factor is introduced in the derived scheme using the theory of singular perturbations. Thomas algorithm is employed to solve the resulting tri-diagonal system of equations. The convergence of the presented method is investigated. Several model example problems are solved using the proposed method. The results are presented with terms of maximum absolute errors, which demonstrate the accuracy and efficiency of the method. It is observed that the proposed method is capable of producing highly accurate results with minimal computational effort for a fixed value of step size  $h$ , when the perturbation parameter tends to zero. From the graphs, we also observed that a numerical solution approximates the exact solution very well in the boundary layers for smaller value of  $\epsilon$ .

**AMS subject classifications (2020):** Primary AMS 65L10; Secondary 65L11, 65L12, 65L20.

\*Corresponding author

Received 22 June 2023; revised 12 August 2023; accepted 14 August 2023

Narendra Kumar

Department of Mathematics, National Institute of Technology Patna, Patna - 800005, India.

e-mail: narendra.ma18@nitp.ac.in

Rajesh Kumar Sinha

Department of Mathematics, National Institute of Technology Patna, Patna - 800005, India.

e-mail: rajesh@nitp.ac.in

Rakesh Ranjan

Department of Science and Technology, Bihar, Government Polytechnic, Lakhisarai, Lakhisarai- 811311, India.

e-mail: 90.ranjan@gmail.com

**Keywords:** Singular perturbation problem; Stability and convergence; Finite difference method.

## 1 Introduction

Singular perturbation problems are of mainly deal in fluid mechanics and other areas of practical/applied mathematics. The solution of the singularly perturbed boundary value problems (BVPs) has a multi-scale nature. The solution varies rapidly in some parts of the domain and varies slowly in some other parts of the domain. The numerical solution of singular perturbation problems (SPPs) is far from trivial, because of the boundary layer behavior of the solution. There are many physical situations in which the sharp changes occur inside the domain of interest, and the narrow regions across which these changes take place are usually referred as Navier–Stokes flow problems, involving high Reynolds number [4, 17, 28], mathematical models of liquid crystal materials and chemical reactions, control theory, and electrical networks [6, 7, 30]. These quick shifts can be managed by fast scales, magnified scales, or stretched scales, but not by slow scales. The domain of integration is typically divided into two subdomains, with a distinct scheme being applied to each subdomain as a common approach to solving this type of problem. In recent years, a large number of analytical methods have been proposed (see [22, 21, 2, 20, 19, 11, 16, 29]). Numerical methods based schemes with and without fitting factors on boundary value techniques and initial value techniques are given in [9, 1, 12, 13, 23, 14]. Phaneendra and Lalu[24] presented Gaussian quadrature for two-point singularly perturbed BVPs with the exponential fitting with a layer at one endpoint, dual boundary layers, and internal boundary layers. In this paper, the given BVP is reduced into an equivalent first-order differential equation with the perturbation parameter as a deviating argument. Then, the Gaussian two-point quadrature technique with exponential fitting is implemented to solve the first-order equation with deviating parameters. Mishra and Saini [18] studied the Liouville–Green transform to solve a singularly perturbed two-point BVP with a right-end boundary layer. Articles [3, 5, 8, 9, 31] proposed different numerical approaches combining fitted mesh methods and fitted operator methods employed by several researchers for solving SPPs, whereas Kadalbajoo and Kumar [10] presented a detailed outline on the numerical methods for solving SPPs. Indeed these existing numerical methods are mostly based on fitted operator techniques or use reasonable theoretical information regarding the solutions, which forms a limitation of these approaches. An efficient method of numerical integration for a class of singularly perturbed two-point BVPs at one endpoint (either left or right) has been presented in [25]. Ranjan, Prasad, and Alam [27] developed a simple method of numerical integration for a class of singularly perturbed two-point BVPs at one endpoint (either left or right). Ranjan and Prasad [26] proposed a fitted finite

difference scheme for solving singularly perturbed two-point BVPs having boundary layer at left or right endpoints. Madhu Latha, Phaneendra, and Reddy [15] presented a numerical solution of SPP using numerical integration with an exponential fitting factor.

In view of the wealth of literature on SPPs, we raise the question of whether there are other ways to attack SPPs, namely ways that are very easy to use and ready for computer implementation. In response to this need for a fresh approach to SPPs, we propose and illustrate in this paper a fitted finite difference technique for singularly perturbed two-point BVPs with a boundary layer on the left (or right) end of the underlying interval. Numerical experience with several linear examples is described.

The paper is organized as follows: Section 2 presents the description of the presented new effective method to solve a second-order singularly perturbed two-point BVP. In Section 3, the convergence of the presented method is investigated. To demonstrate the accuracy and efficiency of the presented method, numerical experiments are carried out for several model test problems, and the results are shown in tables in Section 4. Finally, the discussions and conclusions are presented in the last section 5.

## 2 Statement of the problems

Consider the singularly perturbed two-point BVPs of the following type:

$$\varepsilon v''(t) + r(t)v'(t) + s(t)v(t) = \psi(t) \text{ on } \Omega = [0, 1], \quad (1)$$

subject to the boundary conditions and interval conditions,

$$v(0) = \alpha, \quad v(1) = \beta, \quad (2)$$

where  $\varepsilon$  is a small positive perturbation parameter ( $0 < \varepsilon \ll 1$ ). Furthermore, the functions  $r(t)$ ,  $s(t)$ , and  $\psi(t)$  are continuously differentiable functions in  $[0, 1]$ , where  $\alpha$  and  $\beta$  are constant. In the scenario where we assume that  $r(t) \geq M > 0$  holds true for the entire interval  $[0, 1]$ , with  $M$  representing a positive constant, the boundary layer is expected to occur in the vicinity of  $t = 0$ . On the other hand, if we consider that  $r(t) \leq M < 0$  holds throughout the interval  $[0, 1]$ , with  $M$  being a negative constant, then the boundary layer is anticipated to be located near  $t = 1$ .

## 2.1 Description of the method for left-end boundary layer problems

In this subsection, we describe the proposed method for the solution of the problem (1)–(2) having boundary layer at left-end point of the interval considered.

The solution of (1) with (2) is of the following form (see . 22–261[22]):

$$v(t) = v_0(t) + \frac{r(0)}{r(t)} (\alpha_0 - v_0(0)) e^{-\int_0^t \left(\frac{r(t)}{\varepsilon} - \frac{s(t)}{r(t)}\right) dt} + o(\varepsilon), \quad (3)$$

where  $v_0(t)$  denotes the simplified problem's solution:

$$r(t)v_0'(t) + s(t)v_0(t) = \psi(t), \quad v_0(1) = \beta. \quad (4)$$

By considering the Taylor series expansions of  $r(t)$  and  $s(t)$  around the point  $t = 0$  up to their respective first terms, we can simplify (3) as follows:

$$v(t) = v_0(t) + (\alpha_0 - v_0(0)) e^{-\left(\frac{r(0)}{\varepsilon} - \frac{s(0)}{r(0)}\right)t} + o(\varepsilon). \quad (5)$$

Taking the limit as  $h \rightarrow 0$  and applying (3) to the point  $t = t_i = ih$ ,  $i = 0, 1, 2, \dots, N$ , we obtain

$$\lim_{h \rightarrow 0} v(ih) = v_0(0) + (\alpha_0 - v_0(0)) e^{-\left(\frac{r^2(0) - \varepsilon s(0)}{r(0)}\right)i\rho} + o(\varepsilon), \quad (6)$$

where  $\rho = h/\varepsilon$ , the first and second-order approximations have been used as below:

$$v_i' = \frac{3v_{i+1} - 2v_i - v_{i-1}}{4h}, \quad (7)$$

$$v_i'' = \frac{v_{i+1} - 2v_i + v_{i-1}}{h^2}. \quad (8)$$

Substituting (7) and (8) in (1), we have

$$\varepsilon \left[ \frac{v_{i+1} - 2v_i + v_{i-1}}{h^2} \right] + r_i \left[ \frac{3v_{i+1} - 2v_i - v_{i-1}}{4h} \right] + s_i v_i = \psi_i. \quad (9)$$

Introducing the fitting factor  $\sigma(\rho)$  into the aforementioned approach, we obtain the following result:

$$\sigma\varepsilon \left[ \frac{v_{i+1} - 2v_i + v_{i-1}}{h^2} \right] + r_i \left[ \frac{3v_{i+1} - 2v_i - v_{i-1}}{4h} \right] + s_i v_i = \psi_i. \quad (10)$$

The determination of the fitting factor  $\sigma(\rho)$  aims to ensure that the solution of the difference scheme described in (10) achieves uniform convergence towards the solution of (1) with (2).

By multiplying (10) by  $h$  and considering the limit as  $h \rightarrow 0$ , the result of (10) is as follows:

$$\frac{\sigma}{\rho} [v_{i+1} - 2v_i - v_{i-1}] + \frac{r(0)}{4} [3v_{i+1} - 2v_i - v_{i-1}] = 0. \quad (11)$$

Let  $\mu = \frac{r^2(0) - \varepsilon s(0)}{r(0)}$ . By using (6), we get

$$\begin{aligned} \lim_{h \rightarrow 0} (v(ih - h) + v(ih + h) - 2v(ih)) &= (\alpha_0 - v_0(0)) e^{-\mu i \rho} (e^{\mu \rho} + e^{-\mu \rho} - 2), \\ \lim_{h \rightarrow 0} (3v(ih + h) - 2v(ih) - v(ih - h)) &= (\alpha_0 - v_0(0)) e^{-\mu i \rho} (3e^{-\mu \rho} - 2 - e^{\mu \rho}). \end{aligned}$$

By using the above equations in (11), we get

$$\sigma(\rho) = \frac{r(0)\rho}{2} \coth\left(\frac{(r^2(0) - \varepsilon s(0))\rho}{2r(0)}\right) - \frac{r(0)\rho}{4}, \quad (12)$$

which is a required fitting factor  $\sigma(\rho)$ .

Finally, from (11) with the value of  $\sigma(\rho)$  given by (12), we obtain the following three-term recurrence relationship:

$$P_i v_{i-1} - Q_i v_i + R_i v_{i+1} = H_i \quad (i = 1, 2, 3, \dots, N-1), \quad (13)$$

where

$$\begin{aligned} P_i &= \frac{\sigma \varepsilon}{h^2} - \frac{r_i}{4h}, \\ Q_i &= \frac{2\sigma \varepsilon}{h^2} + \frac{2r_i}{4h} - s_i, \\ R_i &= \frac{\sigma \varepsilon}{h^2} + \frac{3r_i}{4h}, \\ H_i &= \psi_i. \end{aligned}$$

Equation (13) generates an  $(N-1)$  equations system involving  $(N-1)$  undetermined ranging from  $v_1$  to  $v_{N-1}$ . These  $(N-1)$  equations together with the boundary conditions equation (2), are sufficient to solve the obtained tri-diagonal system with the help of an efficient solver called the Thomas algorithm, commonly called as the ‘‘Discrete Invariant Imbedding algorithm’’.

## 2.2 Description of the method for right-end boundary layer problems

In this subsection, we will describe the proposed method for the solution of the problem (1)–(2) having boundary layer at right-end point of the interval considered.

The solution of (1) with (2) is of the following form . 22–261[22]):

$$v(t) = v_0(t) + \frac{r(0)}{r(t)} (\alpha_0 - v_0(1)) e^{-\int_0^t \left(\frac{r(t)}{\varepsilon} - \frac{s(t)}{r(t)}\right) dt} + o(\varepsilon), \tag{14}$$

where  $y_0(t)$  denotes the simplified problem’s solution:

$$r(t)v_0'(t) + s(t)v_0(t) = \psi(t), \quad v_0(1) = \beta. \tag{15}$$

By considering the Taylor series expansions of  $r(t)$  and  $s(t)$  around the point  $t = 0$  up to their respective first terms, we can simplify (14) as follows:

$$v(t) = v_0(t) + (\alpha_0 - v_0(0)) e^{-\left(\frac{r(1)}{\varepsilon} - \frac{s(1)}{r(1)}\right)t} + o(\varepsilon). \tag{16}$$

Taking the limit as  $h \rightarrow 0$  and applying (3) to the point  $t = t_i = ih, i = 0, 1, 2, \dots, N$ , we obtain

$$\lim_{h \rightarrow 0} v(ih) = v_0(0) + (\alpha_0 - y_0(0)) e^{-\left(\frac{r^2(1) - \varepsilon s(1)}{r(1)}\right)i\rho} + o(\varepsilon), \tag{17}$$

where  $\rho = h/\varepsilon$ .

After multiplying (10) by  $h$  and taking the limit as  $h \rightarrow 0$ , (10) converts into the following form:

$$\frac{\sigma}{\rho} [v_{i+1} - 2v_i - v_{i-1}] + \frac{r(0)}{4} [3v_{i+1} - 2v_i - v_{i-1}] = 0. \tag{18}$$

Let  $\mu = \frac{r^2(0) - \varepsilon s(0)}{r(0)}$ . By using (17), we get

$$\begin{aligned} \lim_{h \rightarrow 0} (v(ih - h) + v(ih + h) - 2v(ih)) &= (\alpha_0 - v_0(1)) e^{-\mu i\rho} (e^{\mu\rho} + e^{-\mu\rho} - 2), \\ \lim_{h \rightarrow 0} (3v(ih + h) - 2v(ih) - v(ih - h)) &= (\alpha_0 - v_0(1)) e^{-\mu i\rho} (3e^{-\mu\rho} - 2 - e^{\mu\rho}). \end{aligned}$$

By substituting the aforementioned equations into (18), we get

$$\sigma(\rho) = \frac{r(0)\rho}{2} \coth\left(\frac{(r^2(1) - \varepsilon s(1))\rho}{2r(1)}\right) - \frac{r(0)\rho}{4}, \tag{19}$$

which is a required fitting factor  $\sigma(\rho)$  for right-end boundary layer problem.

### 3 Convergence analysis

This section focuses on the analysis of the convergence of the method.

**Definition 1** (Consistency). Let

$$\phi_i[v] = L_h v(t_i) - L_\phi v(t_i), \quad i = 1, 2, \dots, N.$$

In this context,  $v$  denotes a smooth function defined on the interval  $I = [0, 1]$ , and  $L_h$  represents the discrete difference operator. Consequently, the difference equation (13)–(2) exhibits consistency with the corresponding differential equation (1)–(2), if

$$|\phi_i[v]| \rightarrow 0 \text{ as } h \rightarrow 0.$$

The quantities  $\phi_i[v], i = 1, 2, 3, \dots, N$  is called the local truncation (or local discretization) errors.

**Definition 2.** The differential equation (13)–(2) is said to possess local  $p$ th-order accuracy when, for suitably smooth data, there exists a positive constant  $C$  that remains independent of  $h$  and  $\varepsilon$  such that

$$\max_{1 \leq i \leq N} |\phi_i[v]| \leq Ch^p.$$

The agreement between the differential equation (13)–(2) and (1)–(2), along with its locally second-order accuracy, is established through the lemma provided below.

**Lemma 1.** If  $v \in C^2(I)$ , then

$$|\phi_i[v]| \leq \max_{t_{i-1} \leq t \leq t_{i+1}} \left\{ \frac{r_i h}{4} |v''| \right\} + O(h^2), \quad i = 1, 2, 3, \dots, N - 1.$$

*Proof.* By definition,

$$\begin{aligned} \phi_i &= \sigma\varepsilon \left\{ \frac{v_{i+1} - 2v_i + v_{i-1}}{h^2} - v''_i \right\} + \left\{ \frac{3v_{i+1} - 2v_i - v_{i-1}}{4h} \right\}, \\ \phi_i &= \sigma\varepsilon \left\{ \frac{h^2}{12} v_i^{iv} + \frac{h^4}{360} v_i^{vi} + \dots \right\} + r_i \left\{ \frac{h}{12} v''_i + \frac{h^2}{3!} y_i''' + \dots \right\}, \\ |\phi_i| &= \max_{t_{i-1} \leq t \leq t_{i+1}} \left\{ \frac{\sigma\varepsilon h^2}{12} |v_i^{iv}| \right\} + \max_{t_{i-1} \leq t \leq t_{i+1}} \left\{ \frac{r_i h}{4} |v''_i| \right\}, \\ |\phi_i| &\leq \max_{t_{i-1} \leq t \leq t_{i+1}} \left\{ \frac{r_i h}{4} |v''_i| \right\} + O(h^2), \\ |\phi_i| &\leq O(h). \quad i = 1, 2, 3, \dots, N - 1. \end{aligned}$$

As a result, the intended outcome is attained.  $\square$

We will now examine the proposed method's convergence across the entire interval range  $0 \leq t \leq 1$ . We write the tridiagonal system (13) in the matrix-vector form

$$WV = D, \tag{20}$$

where  $W = (a_{ij}), 1 \leq i, j \leq N - 1$  is a tridiagonal matrix of order  $N - 1$  with

$$\begin{aligned} a_{i,i-1} &= \sigma\varepsilon - \frac{r_i h}{4}, \\ a_{i,i} &= -2\sigma\varepsilon - \frac{2hr_i}{4} + s_i h^2, \\ a_{i,i+1} &= \sigma\varepsilon + \frac{3hr_i}{4}, \end{aligned}$$

and  $D = (d_i)$  is a column vector with  $d_i = h^2\phi_i$  for  $i = 1, 2, 3, \dots, N - 1$  with local truncation error  $\phi_i$ :

$$|\phi_i| \leq O(h). \tag{21}$$

We also have

$$W\bar{V} - \phi(h) = D, \tag{22}$$

where  $\bar{V} = (\bar{V}_0, \bar{V}_1, \bar{V}_2, \bar{V}_3, \dots, \bar{V}_N)^t$  and  $\phi(h) = (\phi_1(h), \phi_2(h), \phi_3(h), \dots, \phi_N(h))^t$  stands for the local truncation error and the real solution, respectively. (20) and (22) give us

$$W(\bar{V} - V) = \phi(h). \tag{23}$$

Thus the error equation is

$$WE = \phi(h), \tag{24}$$

where  $E = \bar{V} - V = (e_0, e_1, e_2, \dots, e_N)^t$ . If  $S_i^*$  is the total of the components in the  $i$ th row of  $W$ , then

$$\begin{aligned} S_1^* &= \sum_{j=1}^{N-1} a_{1,j} = \frac{-\sigma\varepsilon}{h^2} - \frac{r_1}{4h} + s_1, \\ S_{N-1}^* &= \sum_{j=1}^{N-1} a_{N-1,j} = \frac{-\sigma\varepsilon}{h^2} - \frac{3r_{N-1}}{4h} + s_{N-1}, \\ S_i^* &= \sum_{j=1}^{N-1} a_{i,j} = s_i = B_{i0}. \end{aligned}$$

Since  $0 < \varepsilon \ll 1$ , The matrix  $W$  is irreducible and monotone for sufficiently small  $h$ . As a result,  $W^{-1}$  must exist and contain nonnegative elements. Therefore, we have from (24) that

$$E = W^{-1}\phi(h), \tag{25}$$

$$\|E\| \leq \|W^{-1}\| \|\phi(h)\|. \tag{26}$$

Let  $\bar{a}_{ki}$  represent the  $(ki)$ th components of  $W^{-1}$ . Since  $\bar{a}_{ki} \geq 0$ , we have from the operations on matrices:

$$\sum_{j=1}^{N-1} \bar{a}_{ki} S_j^* = 1, \quad k = 1, 2, \dots, N - 1. \tag{27}$$

Therefore, its follows

$$\sum_{j=1}^{N-1} \bar{a}_{ki} \leq \frac{1}{\min_{0 \leq i \leq N-1} S_i^*} = \frac{1}{B_{i0}} \leq \frac{1}{|B_{i0}|}, \tag{28}$$



for some  $i_0$  between 1 and  $N - 1$ , and  $B_{i_0} = q_{i_0}$ .  
Therefore, from (21), (25), and (27), we get

$$e_j = \sum_{i=1}^{N-1} \bar{a}_{ki} \phi_i(h), \quad j = 1(1)N - 1, \quad (29)$$

which implies

$$e_j \leq \frac{O(h)}{|q_i|}, \quad j = 1(1)N - 1. \quad (30)$$

Consequently, by applying the definitions and (29), we obtain:

$$\|E\| = O(h).$$

This implies that the proposed method is the first-order rate of convergence on uniform mesh. As above, we can apply the same procedure for showing the proposed method is of first-order rate of convergence on uniform mesh for the right layer problem.

#### 4 Numerical illustrations

The effectiveness of the proposed method has been demonstrated by implementing it on the three linear SPPs at left-end boundary layer as well as one problem involving a right-end boundary layer and presented the computational results in the tables in terms of the maximum absolute errors  $E_\varepsilon^N$ . These examples have been chosen because they have been widely discussed in literature. For various values of mesh point  $N$  and perturbation parameter  $\varepsilon$ , the  $E_\varepsilon^N$  are defined by  $E_\varepsilon^N = \max_{0 \leq i \leq N-1} [|v(t_i) - v_i|]$ , where  $v(t_i)$  and  $v_i$  denote the exact and approximate solution, respectively. The double mesh principle is used to calculate the rate of convergence defined as  $r_\varepsilon^N = \log_2 \left( \frac{E_\varepsilon^N}{E_{\frac{\varepsilon}{2}}^N} \right)$ . The proposed method is capable of achieving uniform results, when perturbation parameter  $\varepsilon$  tends to 0 for any fixed value of the mesh size  $h$ .

**Example 1.** First, consider the following homogeneous SPP from [15]:

$$\varepsilon v''(t) + v'(t) - v(t) = 0, \quad t \in [0, 1],$$

with boundary condition  $v(0) = 1$  and  $v(1) = 1$ .

The exact solution is given by

$$v(t) = \frac{(e^{m_2} - 1)e^{m_1 t} + (1 - e^{m_1})e^{m_2 t}}{e^{m_2} - e^{m_1}},$$

where  $m_1 = \frac{(-1 + \sqrt{1 + 4\varepsilon})}{2\varepsilon}$  and  $m_2 = \frac{(-1 - \sqrt{1 + 4\varepsilon})}{2\varepsilon}$ .

The maximum absolute errors for various values of  $N$  and singular perturbation parameter  $\varepsilon$  are presented in Table 1 for example 1. It can be easily observed from Table 1 that the maximum absolute errors tends uniformly, when the singular perturbation parameter  $\varepsilon$  tends to 0, for any fixed value of  $N = 1/h$ . Also, rates of convergence presented in Table 1 show that the proposed scheme is capable of producing almost first-order accurate uniformly convergent solution. In Figure 1, we present our solution and the exact solution for various values of  $\varepsilon$  and a fixed value of  $N$ . Clearly, as shown in the figure, the numerical solution and the exact solution are very close within the boundary layers for smaller values of  $\varepsilon$ .

**Example 2.** Consider the following non-homogeneous SPP involving a constant term  $f(t)$  [25, 15]:

$$\varepsilon v''(t) + v'(t) = 2, \quad t \in [0, 1],$$

with boundary condition  $v(0) = 1$  and  $v(1) = 1$ . The exact solution is given by  $v(t) = 2t + \frac{1-e^{t/\varepsilon}}{e^{t/\varepsilon}-1}$ .

The maximum absolute errors for various values of  $N$  and singular perturbation parameter  $\varepsilon$  are presented in Table 2 for example 2. It can be easily observed from Table 2 that the maximum absolute errors tends uniformly, when the singular perturbation parameter  $\varepsilon$  tends to 0, for any fixed value of  $N = 1/h$ . In Figure 2, we present our solution and the exact solution for various values of  $\varepsilon$  and a fixed value of  $N$ . Clearly, as shown in the figure, the numerical solution and the exact solution are very close within the boundary layers for smaller values of  $\varepsilon$ .

**Example 3.** Consider the following non-homogeneous SPP involving a variable term  $f(t)$  [25, 15]:

$$\varepsilon v''(t) + v'(t) = 1 + 2t, \quad t \in [0, 1],$$

with boundary condition  $v(0) = 1$  and  $v(1) = 1$ . The exact solution is given by  $v(t) = \frac{1-e^{-t/\varepsilon}}{1-e^{1/\varepsilon}}(2\varepsilon - 1) + t(t + 1 - 2\varepsilon)$ .

The maximum absolute errors for various values of  $N$  and singular perturbation parameter  $\varepsilon$  are presented in Table 3 for example 3. It can be easily observed from Table 3 that the maximum absolute errors tends uniformly, when the singular perturbation parameter  $\varepsilon$  tends to 0, for any fixed value of  $N = 1/h$ . Also, rates of convergence presented in Table 3 show that the proposed scheme is capable of producing almost first-order accurate uniformly convergent solution. In Figure 3, we present our solution and the exact solution for various values of  $\varepsilon$  and a fixed value of  $N$ . Clearly, as shown in the figure, the numerical solution and the exact solution are very close within the boundary layers for smaller values of  $\varepsilon$ .

**Example 4.** Lastly, consider the following homogeneous SPP at right-end boundary layer [25, 26, 15]:

$$\varepsilon v''(t) - v'(t) - (1 + \varepsilon)v(t) = 0, \quad t \in [0, 1],$$

with boundary condition  $v(0) = 1 + \exp(-(1 + \varepsilon)/\varepsilon)$  and  $v(1) = 1 + 1/e$ . The exact solution is given by  $v(t) = e^{(1+\varepsilon)(t-1)/\varepsilon} + e^{-t}$ .

The maximum absolute errors for various values of  $N$  and singular perturbation parameter  $\varepsilon$  are presented in Table 4 for Example 4. It can be easily observed from the Table 4 that the maximum absolute errors tends uniformly, when the singular perturbation parameter  $\varepsilon$  tends to 0, for any fixed value of  $N = 1/h$ . Also, rates of convergence presented in Table 4 show that the proposed scheme is capable of producing almost first-order accurate uniformly convergent solution. In Figure 4, we present our solution and the exact solution for various values of  $\varepsilon$  and a fixed value of  $N$ . Clearly, as shown in the figure, the numerical solution and the exact solution are very close within the boundary layers for smaller values of  $\varepsilon$ .

Table 1: Computational results in terms of maximum absolute errors for various values of  $N$  and  $\varepsilon$  and the rate of convergence  $r_\varepsilon^N$  for Example 1

N	16	32	64	128	256	512
$\varepsilon = 10^{-5}$	0.0112	0.0057	0.0029	0.0014	0.0007	0.0003
$r_\varepsilon^N$	0.9745	0.9749	1.0506	1.0000	1.2224	
$\varepsilon = 10^{-6}$	0.0112	0.0057	0.0029	0.0014	0.0007	0.0003
$r_\varepsilon^N$	0.9745	0.9749	1.0506	1.0000	1.2224	
$\varepsilon = 10^{-7}$	0.0112	0.0057	0.0029	0.0014	0.0007	0.0003
$r_\varepsilon^N$	0.9745	0.9749	1.0506	1.0000	1.2224	
$\varepsilon = 10^{-8}$	0.0112	0.0057	0.0029	0.0014	0.0007	0.0003
$r_\varepsilon^N$	0.9745	0.9749	1.0506	1.0000	1.2224	
$\varepsilon = 10^{-9}$	0.0112	0.0057	0.0029	0.0014	0.0007	0.0003
$r_\varepsilon^N$	0.9745	0.9749	1.0506	1.0000	1.2224	

Table 2: Computational results in terms of maximum absolute errors for various values of  $N$  and  $\varepsilon$  for Example 2

N	16	32	64	128	256	512
$\varepsilon = 10^{-5}$	0.0000	0.0000	0.0000	0.0000	0.0000	0.0000
$\varepsilon = 10^{-6}$	0.0000	0.0000	0.0000	0.0000	0.0000	0.0000
$\varepsilon = 10^{-7}$	0.0000	0.0000	0.0000	0.0000	0.0000	0.0000
$\varepsilon = 10^{-8}$	0.0000	0.0000	0.0000	0.0000	0.0000	0.0000
$\varepsilon = 10^{-9}$	0.0000	0.0000	0.0000	0.0000	0.0000	0.0000

Table 3: Computational results in terms of maximum absolute errors for various values of  $N$  and  $\varepsilon$  and the rate of convergence  $r_\varepsilon^N$  for Example 3

N	16	32	64	128	256	512
$\varepsilon = 10^{-5}$	0.0586	0.0303	0.0154	0.0079	0.0039	0.0019
$r_\varepsilon^N$	0.9516	0.9764	0.9630	1.0184	1.0375	
$\varepsilon = 10^{-6}$	0.0586	0.0303	0.0154	0.0077	0.0039	0.0019
$r_\varepsilon^N$	0.9516	0.9764	1.0000	0.9814	1.0375	
$\varepsilon = 10^{-7}$	0.0586	0.0303	0.0154	0.0078	0.0039	0.0019
$r_\varepsilon^N$	0.9516	0.9764	0.9814	1.0000	1.0375	
$\varepsilon = 10^{-8}$	0.0586	0.0303	0.0154	0.0078	0.0039	0.0019
$r_\varepsilon^N$	0.9516	0.9764	0.9814	1.0000	1.0375	
$\varepsilon = 10^{-9}$	0.0586	0.0303	0.0154	0.0078	0.0039	0.0019
$r_\varepsilon^N$	0.9516	0.9764	0.9814	1.0000	1.0375	

Table 4: Computational results in terms of maximum absolute errors for various values of  $N$  and  $\varepsilon$  and the rate of convergence  $r_\varepsilon^N$  for Example 1

N	16	32	64	128	256	512
$\varepsilon = 10^{-5}$	0.0112	0.0057	0.0029	0.0014	0.0007	0.0003
$r_\varepsilon^N$	0.9745	0.9749	1.0506	1.0000	1.2224	
$\varepsilon = 10^{-6}$	0.0112	0.0057	0.0029	0.0014	0.0007	0.0003
$r_\varepsilon^N$	0.9745	0.9749	1.0506	1.0000	1.2224	
$\varepsilon = 10^{-7}$	0.0112	0.0057	0.0029	0.0014	0.0007	0.0003
$r_\varepsilon^N$	0.9745	0.9749	1.0506	1.0000	1.2224	
$\varepsilon = 10^{-8}$	0.0112	0.0057	0.0029	0.0014	0.0007	0.0003
$r_\varepsilon^N$	0.9745	0.9749	1.0506	1.0000	1.2224	
$\varepsilon = 10^{-9}$	0.0112	0.0057	0.0029	0.0014	0.0007	0.0003
$r_\varepsilon^N$	0.9745	0.9749	1.0506	1.0000	1.2224	

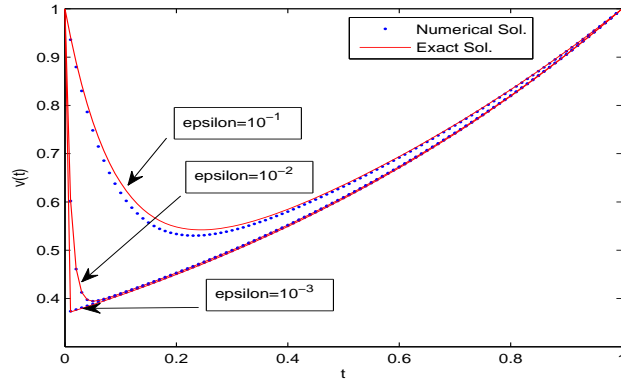


Figure 1: Computational solution of the given Example 1 for the fixed value  $N = 100$  and various values of  $\varepsilon$

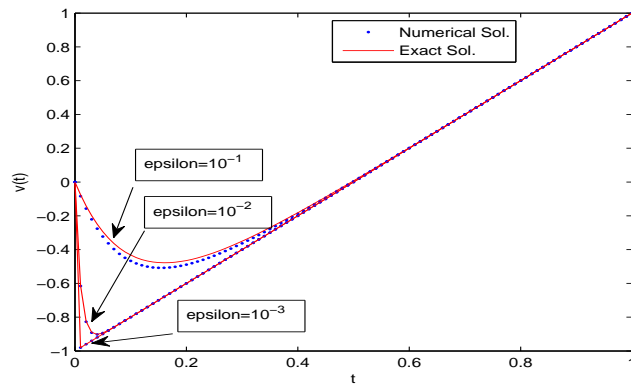


Figure 2: Computational solution of the given Example 2 for the fixed value  $N = 100$  and various values of  $\varepsilon$

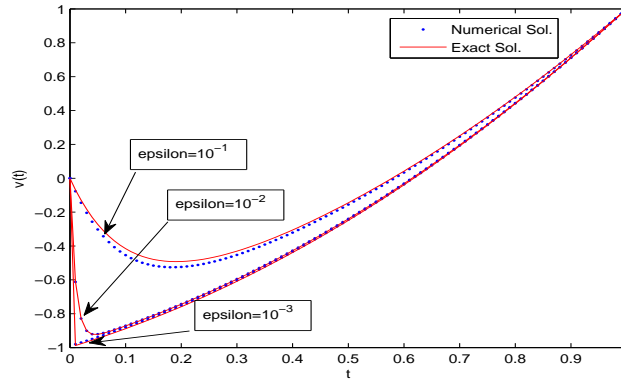


Figure 3: Computational solution of the given Example 3 for the fixed value  $N = 100$  and various values of  $\varepsilon$

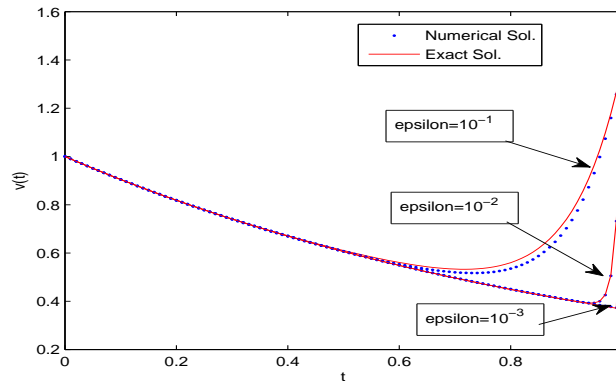


Figure 4: Computational solution of the given Example 4 for fixed value of  $N = 100$  and various values of  $\varepsilon$

### 5 Conclusion

We have derived an exponentially fitted finite difference tridiagonal scheme for solving singularly perturbed two-point BVPs at one endpoint (left or right). We have carried out the convergence analysis for the proposed scheme and performed the numerical experiments on four example problems (three left-end and one right-end problems) for various values of  $N = 1/h$  and perturbation parameter  $\varepsilon$ , which show that the scheme is of almost first-order accurate. The computational results in terms of maximum absolute

error are presented in Tables 1–4. It is easily observed from the tables that the proposed method is capable of producing highly accurate results for a fixed value of mesh size  $h$ , when the perturbation parameter  $\varepsilon$  tends to 0. The maximum absolute errors are becoming uniform for any fixed values of  $N$  when  $\varepsilon \rightarrow 0$ . Furthermore, one can easily observe from Tables 1, 3, and 4 that the proposed exponential fitted finite difference scheme is capable of producing first-order accurate uniformly convergent solution for any fixed value of mesh size  $h = 1/N$  when perturbation parameter  $\varepsilon$  tends to 0. In Figures 1–4, we present our solution and the exact solution for various values of  $\varepsilon$  and a fixed value of  $N$ . Clearly, as shown in the figures, the numerical solution and the exact solution are very close within the boundary layers for smaller values of  $\varepsilon$ . Notably, the novelty of our method lies in its independence from both deviating arguments and fitted meshes [15].

**Conflict of interest** The author declare that he has no competing interests.

## References

- [1] Andargie, A. and Reddy, Y. *Two initial value problems approach for solving singular perturbations problems*, Am. J. Comput. Math. 2(03) (2012), 213–216.
- [2] Bender, C.M. and Orszag, S.A. *Advanced mathematical methods for scientists and engineers*, Springer, New York, 1999.
- [3] Chakravarthy, P. and Reddy, Y.N. *Exponentially fitted modified upwind scheme for singular perturbation problems*, Int. J. Fluid Mech. Res. 33 (2006), 119–136.
- [4] Gold, R.R. *Magneto hydrodynamic pipe flow*, Part I. J. Fluid Mech. 13 (1962), 505–512.
- [5] Habib, H.M. and El-Zahar, E.R. *An algorithm for solving singular perturbation problems with mechanization*, Appl. Math. Comput. 188 (2007), 286–302.
- [6] Hinch, E.J. *Perturbation methods*, Cambridge University Press, Cambridge, 1991.
- [7] Holmes, M.H. *Introduction to perturbation methods*, Springer, Berlin, 1995.
- [8] Jayakumar, J. and Ramanujam, N. *A numerical method for singular perturbation problems arising in chemical reactor theory*, Comput. Math. Appl. 27 (1994,) 83–99.

- [9] Kadalbajoo, M.K. and Kumar, D. *Initial value technique for singularly perturbed two point boundary value problems using an exponentially fitted finite difference scheme*, Comput. Math. Appl. 57 (2009), 1147–1156.
- [10] Kadalbajoo, M.K. and Kumar, D. *A brief survey on numerical methods for solving singularly perturbed problems*, Appl. Math. Comput. 217 (2010), 3641–3716.
- [11] Kevorkian, J. and Cole, J.D. *Perturbation methods in applied mathematics*, 2nd Edition, Springer-Verlag, New York, 1981.
- [12] Kumar, M. and Surabhi, T. *An initial-value technique to solve third-order reaction-diffusion singularly perturbed boundary-value problems*, Int. J. Comput. Math. 89(17) (2012), 2345–2352.
- [13] Kumar, M., Singh, P. and Hradyesk Kumar, M. *An initial-value technique for singularly perturbed boundary value problems via cubic spline*, Int. J. Comput. Methods Eng. Sci. Mech. 8(6) (2007), 419–427.
- [14] Lorenz, J. *Combinations of initial and boundary value methods for a class of singular perturbation problems*, Numerical analysis of singular perturbation problems (Proc. Conf., Math. Inst., Catholic Univ., Nijmegen, 1978), pp. 295–315, Academic Press, London-New York, 1979.
- [15] Madhu Latha, K., Phaneendra, K. and Reddy, Y.N. *Numerical integration with exponential fitting factor for singularly perturbed two point boundary value problems*, British Journal of Mathematics & Computer Science 3(3) (2013), 397–414.
- [16] Miller, J.J.H. *Singular perturbation problems in chemical physics, analytic and computational methods*, XCVII Wiley, New York, 1997.
- [17] Miller, J.J.H., Riordan, R.E.O. and Shishkin, G.I. *Fitted numerical methods for singular perturbation problems, error estimates in the maximum norm for linear problems in one and two dimensions*, World Scientific, 1996.
- [18] Mishra, H. and Saini, S. *Numerical solution of singularly perturbed two-point boundary value problem via Liouville-Green transform*, Am. J. Comput. Math. 3(1) (2013), 1–5.
- [19] Nayfeh, A.H. *Perturbation methods*, John Wiley & Sons, Inc., New York, 1979.
- [20] Nayfeh, A.H. *Introduction to perturbation techniques*, Wiley-VCH, New York, 1993.
- [21] O'Malley, R.E. *Introduction to singular perturbations*, Academic Press, New York, 1974.



- [22] O'Malley, R.E. *Singular perturbation methods for ordinary differential equations*, Applied Mathematical Sciences, 89, Springer, Berlin, 1990.
- [23] Padmaja, P., Aparna, P. and Gorla, R.S.R. *An initial-value technique for self-adjoint singularly perturbed two-point boundary value problems*, Int. J. Appl. Mech. Eng. 25(1) (2020), 106–126.
- [24] Phaneendra, K. and Lalu, M. *Gaussian quadrature for two-point singularly perturbed boundary value problems with exponential fitting*, Communications in Mathematics and Applications 10(3) (2019), 447–467.
- [25] Ranjan, R. and Prasad, H.S. *An efficient method of numerical integration for a class of singularly perturbed two point boundary value problems*, WSEAS Trans. Math. 17 (2018), 265–273.
- [26] Ranjan, R. and Prasad, H.S., *A fitted finite difference scheme for solving singularly perturbed two point boundary value problems*, Inf. Sci. Lett. 9(2), (2020), 65–73.
- [27] Ranjan, R., Prasad, H.S. and Alam, J. *A simple method of numerical integration for a class of singularly perturbed two point boundary value problems*, i-manager's Journal on Mathematics 7(1) (2018), 41.
- [28] Roos, H.G., Stynes, M. and Tobiska, L. *Numerical methods for singularly perturbed differential equations*, Springer, Berlin 1996.
- [29] Smith, D.R. *Singular perturbation theory: An introduction with applications*, Cambridge University Press, Cambridge, 1985.
- [30] Verhulst, F. *Methods and applications of singular perturbations: Boundary layers and multiple timescale dynamics*, Springer, Berlin 2005.
- [31] Vigo-Aguiar, J. and Natesan, S. *An efficient numerical method for singular perturbation problems*, J. Comput. Appl. Math., 192 (2006), 132–141.

#### How to cite this article

Kumar, N., Kumar Sinha, R. and Ranjan, R., Singularly perturbed two-point boundary value problem by applying exponential fitted finite difference method. *Iran. J. Numer. Anal. Optim.*, 2023; 13(4): 711-727. <https://doi.org/10.22067/ijnao.2023.83070.1283>